

Thioglycolic acid on the gold (111) surface and Raman vibrational spectra

Jian-Ge Zhou^a, Quinton L. Williams^a, Ruqian Wu^b,

^a*Department of Physics, Atmospheric Sciences, and Geoscience,
Jackson State University, Jackson, MS 39217, USA*

^b*Department of Physics and Astronomy,
University of California, Irvine, California 92697-4575, USA*

Abstract

The interaction of thioglycolic acid (HSCH_2COOH) with the Au(111) surface is investigated, and it is found that at the low coverage the molecule lies down on the substrate. If the mercaptan-hydrogen atom is eliminated, the resulting SCH_2COOH molecule is randomly oriented on the surface. If the carboxylic acid group in the HSCH_2COOH molecule is deprotonated instead, the $\text{HSCH}_2\text{COO}^-$ molecule lies down on the surface. However, when the mercaptan-hydrogen atom in the $\text{HSCH}_2\text{COO}^-$ molecule is removed, the resulting SCH_2COO^- molecule rises up to a certain level on the substrate. The calculated Raman vibrational spectra decipher which compounds and atomic displacements contribute to the corresponding frequencies. We thus propose a consistent mechanism for the deposition of thioglycolic acid on the Au(111) surface.

PACS numbers: 68.43.Bc, 61.43.Bn, 73.20.Hb

I. INTRODUCTION

Self-assembled monolayers (SAMs) have attracted considerable attention as model systems for many fundamental and technological investigations¹. The thiol and thiolate-based SAMs have broad applications on supramolecular assembly, wetting, tribology, corrosion inhibition, lithography, chemical and biochemical sensors, optics, and immobilization of DNA, because of both their simplicity and stability. In particular, SAMs can simulate a biological membrane which allows adsorption of proteins to metal surfaces without denaturation²⁻⁴. The peptide molecules with some enzymatic activity can be deposited on metal surfaces via the thiol or thiolate linkage monolayer^{5,6}. The deposition of a second monolayer on the top of the first adsorbed thiol or thiolate monolayer yields a bilayer system consisting of two monomolecular films. In other words, a layer of peptide molecules can be bonded to the gold surface via the linkage monolayer formed from the thioglycolic acid (HSCH_2COOH)⁵⁻⁷.

The chemisorption of the thioglycolic acid on the gold surface was demonstrated using surface-enhanced Raman scattering⁸ and ultrafast electron crystallography⁹. It was found when the higher portion of the carboxylic acid groups is deprotonated, the higher portion of the thioglycolic acid molecules adopts a trans conformation⁸. It was also observed that after 2,2'-dithiodiacetic acid is deposited on the Au(111), the SCH_2COOH molecules are randomly oriented on the gold surface⁹, that is, the adsorption pattern related to the SCH_2COOH is different from that corresponding to the HSCH_2COOH . On the other hand, the switchable SAM under the influence of an electrical potential was observed with intentionally created room for conformational changes of the molecules¹⁰. When the external electrical potential is turned on, the hexadecanoic acid molecules ($\text{HS}(\text{CH}_2)_{15}\text{COO}^-$) bend their negatively charged COO^- group towards to the positively charged gold surface¹⁰. Simulating this switchable SAM process via the *ab initio* method requires a prohibitive amount of computer time, so one has to study the simple case: the $\text{HSCH}_2\text{COO}^-$ on the Au(111) surface.

It was recently observed that thiol stays intact when deposited on the regular Au(111) surface, but the S-H bond of the thiol is broken on the defected Au(111) surface^{11,12}. Upon the HSCH_2COOH molecules deposit on the Au(111), they can either remain intact, or turn into one of the following substances: 1) SCH_2COOH in the presence of the defect on the Au(111)^{11,12}; 2) $\text{HSCH}_2\text{COO}^-$ by increasing pH value⁸; 3) SCH_2COO^- by the defect and increasing pH value. To get a consistent picture of the thioglycolic acid adsorption on the

Au(111), one has to examine the adsorption patterns of the HSCH₂COOH, SCH₂COOH, HSCH₂COO⁻, and SCH₂COO⁻ on the Au(111) separately. Even some theoretical simulations on thiol or thiolate based SAMs have been carried out¹³⁻²⁰, however, there has been no first-principle calculation which provides an atomic-scale description of the HSCH₂COOH, SCH₂COOH, HSCH₂COO⁻, and SCH₂COO⁻ on the Au(111) surface. The electronic properties for this system, such as the projected density of states (PDOS) and the charge density difference, have not been discussed. While a large variety of thiol or thiolate based SAMs has been studied, still little is known about why the SCH₂COOH molecules are randomly oriented on the gold surface, and how the HSCH₂COOH molecules orient on the Au(111). Thus theory is challenged to propose a consistent model for the thioglycolic acid adsorption process on the Au(111) surface.

In this contribution, we address the adsorption patterns of the HSCH₂COOH, SCH₂COOH, HSCH₂COO⁻ and SCH₂COO⁻ molecules on the Au(111) surface from first principle calculation. We present adsorption energies and geometries for these four kinds of molecules on the Au(111) surface at 0.25 ML, and find that they demonstrate different adsorption patterns. We calculate the partial density of states (PDOS) projected on the S and O2 atom (with an attached hydrogen, see Fig. 1) to show their relation to the adsorption patterns, and evaluate the charge-density differences to illustrate the interacting bond between the adsorbates and the Au(111). We also compute the Raman vibrational spectra of these four kinds of molecules adsorbed on the surface to decipher the adsorption mechanism of the thioglycolic acid on the Au(111) substrate. By the comparison of the experimental frequencies with the computational ones, we can identify which compounds and atomic displacements contribute to the corresponding frequencies. We thus reveal how the dissociation of the mercaptan hydrogen atom and the deprotonation of carboxylic acid group play key roles in the adsorption process, and propose a consistent mechanism for the deposition of thioglycolic acid on the Au(111) surface.

II. COMPUTATIONAL METHOD

The calculations were carried out in the slab model with periodic boundary conditions by density functional theory (DFT)^{21,22}. The electron-ion interaction has been described using the projector augmented wave (PAW) method^{23,24}. All calculations have been performed by

Perdew-Wang 91 (PW91) generalized gradient approximation²⁵. The wave functions were expanded in a plane wave basis with an energy cutoff of 400 eV. The k points were obtained from Monkhorst-Pack scheme²⁶, and $3 \times 3 \times 1$ k point mesh was for the geometry optimization. The optimization of the atomic geometry was performed via conjugate-gradient minimization of the total energy with respect to the atomic coordinates. The supercell consisted of five layers with each layer having 12 Au atoms. The Au atoms in the top three atomic layers are allowed to relax, while those in the bottom two layers are fixed to simulate bulk-like termination²⁷. The vacuum region comprises ten atomic layers, which exceeds substantially the extension of the thioglycolic acid molecule²¹. For charged systems, a uniform compensating background is incorporated to maintain the charge neutrality of the supercell²⁸. The harmonic approximation was applied to calculate the Hessian matrix and vibrational frequencies. We calculated the gold lattice constant and found it to agree with the experimental value²⁹ within 2.1%.

III. RESULTS AND DISCUSSION

In this section, we discuss the adsorption pattern of the HSCH₂COOH, SCH₂COOH, HSCH₂COO⁻, and SCH₂COO⁻ on the Au(111) substrate, respectively. The adsorption energy of the system is defined as $E_{ads} = E_{adsorbate} + E_{Au(111)} - E_{adsorbate+Au(111)}$. The symbol top-fcc (or top-hcp) in the following tables represents the S atom being on the atop site of the gold atom, but leaned toward the fcc (or hcp) hollow center, and analogously for the notations bri-fcc, bri-hcp, etc. The units for the bond length and adsorption energy are Angstrom (Å) and eV.

A. The HSCH₂COOH molecule on the Au(111) surface

First, let us begin with our analysis with the geometries and adsorption energies of the optimized structures for the thioglycolic acid on the Au(111) surface at the coverage of 0.25 ML, as displayed in Table I. Here 1.00 ML means one sulfur per three gold atoms, and 0.25ML stands for one thioglycolic acid on a gold surface with twelve gold atoms. In Table I, the entries θ , *tilt direct* and d_{S-Au} refer to the polar angle between the normal vector of the surface and the S-C2 direction, the Au(111) surface region towards which the S-C2 is

TABLE I: The geometries and adsorption energies for the structures of thioglycolic acid on Au(111) at 0.25ML. The entries θ , *tilt direct* and d_{S-Au} refer to the polar angle between the normal vector of the surface and the S-C2 direction, the Au(111) surface region towards which the S-C2 is tilted, and the shortest Au-S bond length. The entries *initial* and *optimized site* stand for the S atom attachment site before and after optimization. The maximum adsorption energy is underlined.

initial site	θ	d_{S-Au} Å	optimized site	θ deg	tilt direct	d_{S-Au} Å	E_{ads} eV
bri	0	2.60	bri	2.9	hcp	2.97	0.27
	45	2.60	bri-fcc	54.8	hcp	2.89	0.45
	90	2.60	bri	86.9	hcp	3.16	0.47
fcc	0	2.60	bri-fcc	9.7	hcp	2.98	0.32
	45	2.60	bri-fcc	61.0	hcp	3.11	0.36
	90	2.60	top-fcc	83.7	hcp	3.18	0.50
hcp	0	2.60	bri-hcp	5.8	fcc	2.95	0.30
	45	2.60	bri-hcp	54.2	fcc	2.87	0.48
	90	2.60	hcp	89.4	fcc	3.58	0.44
top	0	2.60	top	8.0	hcp	2.93	0.26
	45	2.60	top	54.8	hcp	2.81	0.37
	90	2.60	top	74.2	fcc	2.57	<u>0.63</u>

tilted, and the shortest Au-S bond length, respectively. The entries *initial* and *optimized site* stand for the S atom attachment site before and after optimization. The columns 1-3 and 4-7 list structural data pertaining to the initial and the final optimized geometry. The maximum adsorption energy is underlined.

Table I shows the adsorption energy for the most stable structure of the HSCH₂COOH on the Au(111) surface is 0.63 eV, and the adsorption site preferred by the sulfur atom is located at the atop site of the gold atom. This stable configuration is illustrated in Fig. 1a. The polar angle between the normal vector of the surface and the S-C2 direction is 74.2°. Fig. 1a indicates that at the low coverage, the HSCH₂COOH tends to lie down⁸. The S-Au bond length is 2.57 Å, which suggests that the bonding between the S atom in the

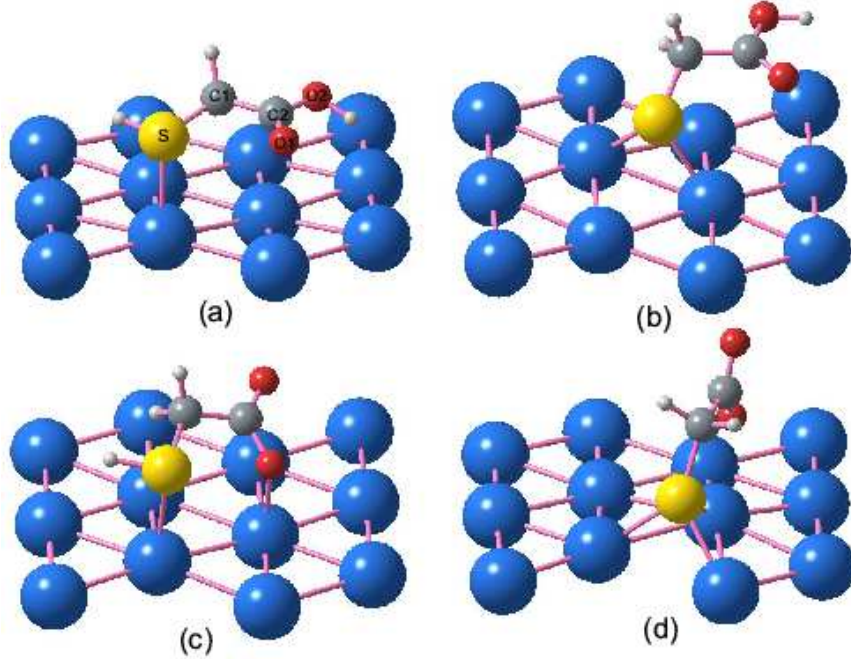


FIG. 1: (a) The thioglycolic acid (HSCH_2COOH) on the Au(111) surface. (b) SCH_2COOH on the surface. (c) $\text{HSCH}_2\text{COO}^-$ on the surface. (d) SCH_2COO^- on the surface.

HSCH_2COOH and the gold atom could be described as chemisorption¹¹.

B. The SCH_2COOH molecule on the gold substrate

Ruan et al. used 2,2'-dithiodiacetic acid to make SAMs on the gold surface⁹, then the SCH_2COOH is deposited on the surface. The SCH_2COOH can also be obtained from the HSCH_2COOH molecule by taking away the mercaptan hydrogen atom which is initially attached to the sulfur. The adsorption pattern of the SCH_2COOH molecule on the Au(111) surface is depicted in Table II. The adsorption energy for the most stable configuration of the SCH_2COOH on the Au(111) surface in Table II is 2.34 eV, and the favored adsorption site by the sulfur atom is in the hcp hollow center, but leaned to the Au-Au bridge. The corresponding structure is shown in Fig. 1b. The sulfur atom forms bonds with two Au atoms, and the S-Au bond length is 2.47 Å. The angle between the normal vector of the surface and the S-C2 direction is 68.0°. However, in Table II there are two configurations marked by # (bri-45° and hcp-45°) with adsorption energies 2.33 eV, which is close to the energy of the most stable one (2.34 eV). The corresponding angles θ for these two #

TABLE II: The geometries and adsorption energies for the structures of the SCH₂COOH molecule on the Au(111) at 0.25ML.

initial site	θ	d_{S-Au} Å	optimized site	θ deg	tilt direct	d_{S-Au} Å	E_{ads} eV
bri	0	2.60	bri-hcp	6.5	fcc	2.48	2.26
	#45	2.60	bri-fcc	46.1	hcp	2.45	2.33
	90	2.60	bri-fcc	71.3	hcp	2.42	2.17
fcc	0	2.60	fcc	9.8	hcp	2.47	2.28
	45	2.60	fcc	51.0	hcp	2.51	2.17
	90	2.60	bri-fcc	71.3	hcp	2.50	2.23
hcp	0	2.60	bri-hcp	2.7	fcc	2.47	2.22
	#45	2.60	bri-hcp	41.6	fcc	2.46	2.33
	90	2.60	bri-hcp	68.0	fcc	2.47	<u>2.34</u>
top	0	2.60	top-fcc	10.1	hcp	2.40	2.01
	45	2.60	top-fcc	63.0	hcp	2.40	1.89
	90	2.60	top-fcc	70.3	hcp	2.59	2.05

marked configurations are 46.1° and 41.6°, respectively. This can be interpreted as when the SCH₂COOH molecules are deposited on the Au(111) surface, some SCH₂COOH molecules lie on the substrate (see Fig. 1b), but some of them rise up to a certain level (corresponding to # marked configurations). Thus in the case of SCH₂COOH, the configurations with different tilted angles may admix, and the molecule appears to deposit on the gold substrate randomly⁹.

C. The HSCH₂COO⁻ molecule on the surface

When the thioglycolic acid is adsorbed on the Au(111) surface, its carboxylic acid group (COOH) can be deprotonated and it becomes HSCH₂COO⁻⁸. The optimized adsorption configurations of the HSCH₂COO⁻ molecule on the Au(111) surface are described in Table III. The adsorption energies in Table III demonstrate that the sulfur atom in the

TABLE III: The geometries and adsorption energies for the structures of the HSCH₂COO⁻ molecule on the Au(111) surface at 0.25ML.

initial site	θ	d_{S-Au}	optimized site	θ	tilt	d_{S-Au}	E_{ads}
		\AA		deg	direct	\AA	eV
bri	0	2.60	bri	1.1	hcp	2.86	0.44
	45	2.60	bri	50.6	hcp	2.66	0.67
	90	2.60	bri	82.8	hcp	2.99	0.96
fcc	0	2.60	bri-fcc	8.0	fcc	2.67	0.54
	45	2.60	bri-fcc	65.4	fcc	2.74	0.92
	90	2.60	top-fcc	77.1	hcp	3.38	0.95
hcp	0	2.60	hcp	1.5	fcc	2.75	0.66
	45	2.60	top-hcp	46.6	fcc	2.57	0.81
	90	2.60	bri-hcp	78.0	fcc	3.62	0.83
top	0	2.60	top	5.7	hcp	2.85	0.30
	45	2.60	top	56.6	hcp	2.65	0.94
	90	2.60	top	82.9	hcp	2.60	<u>1.13</u>

HSCH₂COO⁻ molecule prefers to stay on the atop site of the gold atom, as indicated in Fig. 1c. The corresponding adsorption energy is 1.13 eV which is larger than that of the thio-glycolic acid on the Au(111) surface. The S-Au bond length is around 2.60 \AA and the angle θ is 82.9°, which means the HSCH₂COO⁻ molecule is lying down on the gold substrate.

D. The SCH₂COO⁻ molecule on the Au(111) surface

If the mercaptan-H atom in the HSCH₂COO⁻ is detached from the sulfur atom, the resulting compound is the SCH₂COO⁻. Table IV shows that the sulfur atom favors the fcc hollow center with the adsorption energy 2.34 eV. The polar angle between the normal vector of the gold surface and the S-C2 direction is 53.4°; so, after losing mercaptan-H atom, the SCH₂COO⁻ molecules begin to rise, see Fig. 1d. Note that there is a # marked configuration in Table IV, whose adsorption energy is 2.33 eV - very closed to 2.34 eV. The

TABLE IV: The geometries and adsorption energies for the structures of the SCH_2COO^- molecule on the Au(111) surface at 0.25ML.

initial site	θ	d_{S-Au}	optimized site	θ	tilt	d_{S-Au}	E_{ads}
		\AA		deg	direct	\AA	eV
bri	0	2.60	bri-hcp	9.2	fcc	2.51	2.16
	45	2.60	bri	44.9	hcp	2.45	2.01
	90	2.60	bri-fcc	78.6	hcp	2.43	2.21
fcc	0	2.60	fcc	7.8	hcp	2.47	2.14
	45	2.60	bri-fcc	53.4	hcp	2.49	<u>2.34</u>
	90	2.60	bri-fcc	83.2	hcp	2.49	2.28
hcp	0	2.60	hcp	0.5	fcc	2.49	2.11
	45	2.60	bri-hcp	39.8	fcc	2.44	2.04
	90	2.60	bri-hcp	76.4	fcc	2.45	2.27
top	0	2.60	bri-top	10.1	bri	2.54	1.88
	#45	2.60	bri-hcp	51.8	fcc	2.43	2.33
	90	2.60	top	81.8	fcc	2.38	2.08

angle θ for top-45° structure (the # marked configuration) is 51.8°. The stable structures in Table IV indicate that when the SCH_2COO^- is deposited on the Au(111) surface, the molecule rises up to a certain level⁸ (see Fig. 1d).

E. Electronic Structures

To understand how the dissociation of the mercaptan-hydrogen atom and the deprotonation of the carboxylic acid group play roles in the adsorption process, we calculate the partial density of states (PDOS) projected on the S and O2 atoms in the HSCH_2COOH , SCH_2COOH , $\text{HSCH}_2\text{COO}^-$, SCH_2COO^- molecule deposited on the Au(111) substrate. There are three sharp peaks in the PDOS projected on the S atom in the isolated HSCH_2COOH molecule (Fig. 2a). The major contributions of three peaks come from π , σ and π^* orbitals in the S-C bond. To calibrate the Fermi level for the isolated molecule,

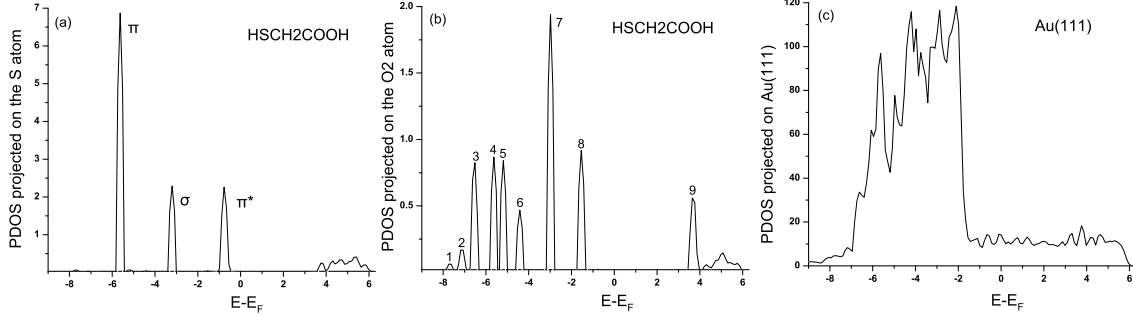


FIG. 2: (a)-(b) PDOS projected on the S and O2 atom in the isolated HSCH₂COOH, (c) DOS for a pure Au(111) surface.

in the calculation we have separated the HSCH₂COOH molecule from the gold surface by 8Å so that there is no interaction between the molecule and the substrate. The corresponding PDOS projected on the S atom can be regarded as that in the isolated HSCH₂COOH molecule. The density of states for the pure gold surface vanishes above 6eV (Fig. 2c). The π^* orbital is located on the right edge of the Au d band, the π orbital is near the left edge of the Au d band, whereas the σ orbital overlaps with the gold d band (Fig. 2a, Fig. 2c). Upon the HSCH₂COOH molecule is deposited on the surface (Fig. 3a), the σ and π^* states disperse as a consequence of the mixing with the gold d states, whereas π orbital remains sharp and shifts toward more negative energy. The adsorption energy of 0.63eV indicates that the major interaction between the sulfur in the HSCH₂COOH molecule and the gold surface is not van der Waals force, so Fig. 3a might not have the signature of the weak bond.

If the mercaptan-hydrogen atom is dissociated from the S atom, the π state splits indicating a stronger S-Au bonding interaction originating from the hybridization of the π orbital of the SCH₂COOH with the gold d band (Fig. 3b). The PDOS projected on the S atom is insensitive to the deprotonation of the carboxylic acid group, which explains why the profiles of Fig. 3a and Fig. 3c are similar so are Fig. 3b and Fig. 3d. No energy gap in the PDOS projected on the S atom attached to the Au(111) surface (Fig. 3a-3d). This is because the HOMO and LUMO level of the S atom fall into the energy range of the gold d-band with a concomitant hybridization, that is, the PDOS projected on the S atom near the Fermi level is dominated by d-states from the Au(111) surface. The effect of the deprotonation of the carboxylic acid group is demonstrated by the PDOS projected on the O2 atom (Fig.

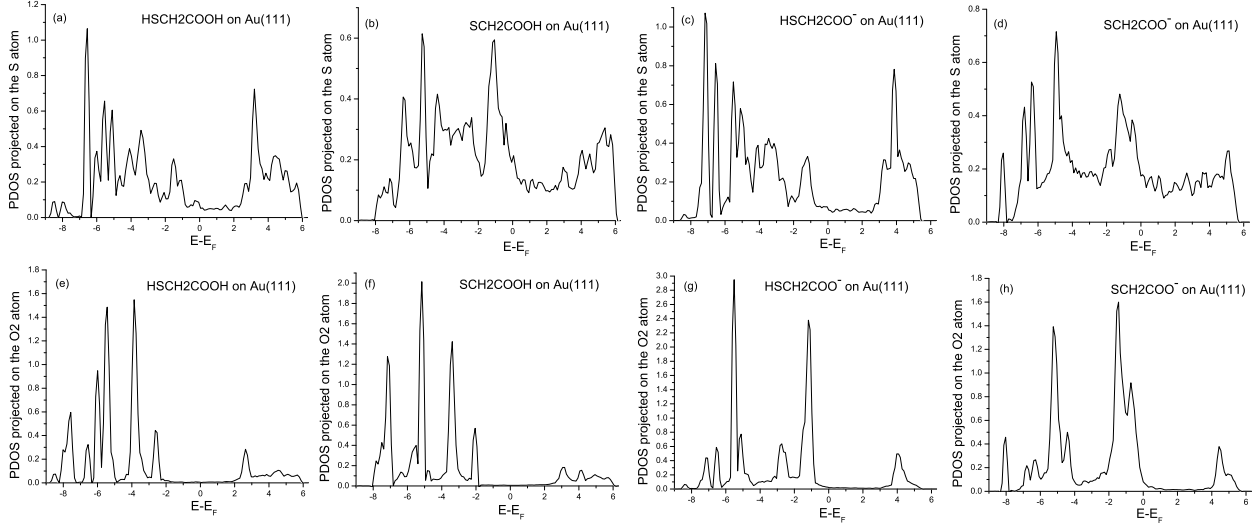


FIG. 3: (a)-(d) PDOS on the S in the HSCH₂COOH, SCH₂COOH, HSCH₂COO⁻ and SCH₂COO⁻ on the surface, (e)-(h) PDOS on the O2 in the HSCH₂COOH, SCH₂COOH, HSCH₂COO⁻ and SCH₂COO⁻ on the surface.

3e-Fig. 3h). Nine sharp peaks are illustrated in the PDOS projected on the O2 atom in the isolated HSCH₂COOH molecule (Fig. 2b). Upon the HSCH₂COOH is deposited on the gold surface, some peaks are suppressed (Fig. 3e), however, the PDOS projected on the O2 atom is insensitive to the adsorption and the dissociation of the mercaptan-hydrogen atom (Fig. 3e, Fig. 3f). Fig. 3g and Fig. 3h show that some peaks in Fig. 2b disappear and some others disperse after the carboxylic acid group is deprotonated, which indicates that the deprotonation changes the electronic states around the O2 atom.

To further elucidate the interacting bond between the HSCH₂COOH, SCH₂COOH, HSCH₂COO⁻, SCH₂COO⁻ molecule and the Au(111) substrate, we calculate the charge-density difference: $\Delta\rho(\vec{r}) = \rho_{ads/sub}(\vec{r}) - \rho_{sub}(\vec{r}) - \rho_{ads}(\vec{r})$, where $\rho_{ads/sub}$, ρ_{sub} , and ρ_{ads} are the electron charge densities of the relaxed adsorbate-substrate system, of the clean relaxed surface, and of the isolated but adsorptionlike deformed adsorbate (without substrate), respectively. The isodensity surfaces of the charge-density difference for the structures of the HSCH₂COOH, SCH₂COOH, HSCH₂COO⁻, and SCH₂COO⁻ on the Au(111) substrate are depicted in Figs. 4a-4d. In Fig. 4, we display only the surrounding part of the S-Au bond. As we know, two p-electrons of the sulfur in the HSCH₂COOH molecule form a lone pair, and the region around the top of the gold is a charge depletion area³⁰. In the configuration

of Fig. 4a, the sulfur atom sits on the top of the gold atom. The lone pair in the sulfur is attracted to this charge depletion region, and $0.3e$ is transferred from the sulfur lone pair orbital to the gold charge depletion area. Thus when the sulfur atom in the thioglycolic acid is adsorbed on the Au(111) (Fig. 4a), the electrostatic interaction responsible for the bonding comes from the monopole term and the dipole moments in the adsorbate and substrate³¹. Around the sulfur atom, there is a “ring” of accumulation of electron charge. The electrostatic interaction is dominated by the attractive ionic term modified by a repulsive dipolar term³¹. The sulfur atom stays on the top of the gold atom, that is, the S atom only forms a bond with one gold atom. If the mercaptan-hydrogen atom is detached from the sulfur (Fig. 4b), the S-Au bond is largely covalent with some ionic character³². The sulfur in the SCH_2COOH forms bonds with two gold atoms of the Au(111) surface. The interaction between the $\text{HSCH}_2\text{COO}^-$ and the gold surface is the similar to the thioglycolic acid case (Fig. 4c), except that the O1 atom form an additional bond with the gold atom. There is big depletion of electrons around the gold atom. The p_x, p_y orbits in the O1 atom gain extra electrons, but the p_z orbit loses some electrons. Thus, this O1-Au bonding is a convolution between the ionic bond and the covalent bond. Fig. 4d suggests that the S-Au bonds for the SCH_2COO^- is a covalent bond with some ionic character.

F. The adsorption mechanism

From the above discussion, we propose the following picture. When the HSCH_2COOH molecule is adsorbed on the gold substrate, it lies down on the surface⁸ (Fig. 1a). When the 2,2'-dithiodiacetic acid is put on the gold surface, the SCH_2COOH molecules form the SAM on the substrate⁹. If the thioglycolic acid is deposited on the gold surface with defects, the mercaptan hydrogen atom can be dissociated from the S atom and the HSCH_2COOH molecule becomes SCH_2COOH ^{11,12}. Some SCH_2COOH molecules lie down on the substrate (see Fig. 1b), but others rise up to a certain level. Thus, in the case of SCH_2COOH , different configurations may admix and the adsorption appears to be randomly oriented⁹. If the carboxylic acid group in the HSCH_2COOH molecule is deprotonated by increasing the pH value, the resulting $\text{HSCH}_2\text{COO}^-$ lies on the surface (Fig. 1c). However, when the mercaptan hydrogen atom in the $\text{HSCH}_2\text{COO}^-$ molecule is ruptured from the sulfur, the resulting SCH_2COO^- molecule rises up to a certain level⁸ (Fig. 1d).

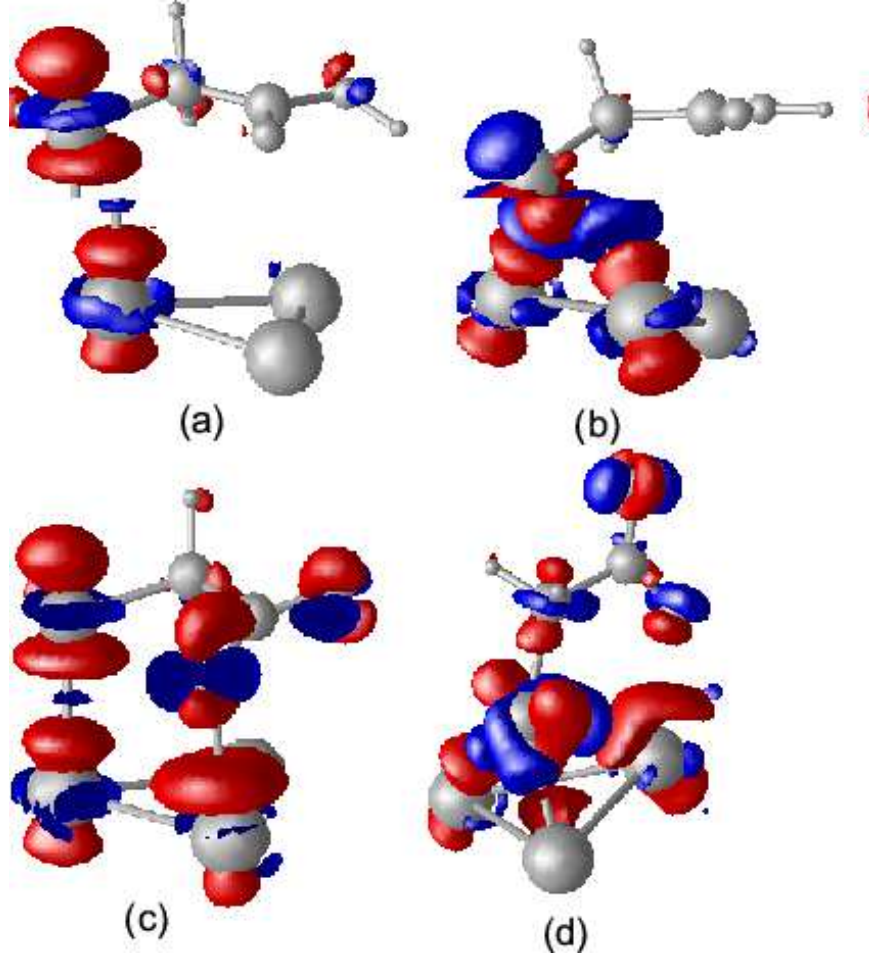


FIG. 4: The isosurfaces of the charge-density difference for (a) the HSCH_2COOH adsorption on the Au(111) surface with blue (accumulation of electrons) and/or red (depletion of electrons) isosurface value, $\pm 0.02e/\text{\AA}^3$, (b) SCH_2COOH on the surface, (c) $\text{HSCH}_2\text{COO}^-$ on the surface, and (d) SCH_2COO^- on the surface. Only three related gold atoms of the Au(111) surface are displayed.

IV. THE RAMAN VIBRATIONAL SPECTRA

To support the above adsorption mechanism, we calculate the Raman vibrational spectra of the HSCH_2COOH , SCH_2COOH , $\text{HSCH}_2\text{COO}^-$ and SCH_2COO^- adsorbed on the Au(111) substrate, respectively. The Raman vibrational peak frequencies (cm^{-1}) for experimental data and computational values for the HSCH_2COOH , SCH_2COOH , $\text{HSCH}_2\text{COO}^-$ and SCH_2COO^- on the Au(111) surface are listed in Table V. The vibrational frequencies

TABLE V: Raman vibrational peak frequencies (cm^{-1}): Experimental data and computational values for the HSCH_2COOH , SCH_2COOH , $\text{HSCH}_2\text{COO}^-$ and SCH_2COO^- on the Au(111) surface. The calculated frequencies which are the closest to the experimental ones are underlined.

frequencies	ω_1	ω_2	ω_3	ω_4	ω_5	ω_6	ω_7	ω_8
Exp. data ⁸	575	665	763	905	930	1387	1597	1711
Au- HSCH_2COOH	<u>575</u>	653	<u>745</u>	<u>881</u>	-	1409	-	<u>1733</u>
Au- SCH_2COOH	596	<u>670</u>	725	872	-	<u>1396</u>	-	1738
Au- $\text{HSCH}_2\text{COO}^-$	592	619	734	-	<u>929</u>	1369	1627	-
Au- SCH_2COO^-	598	638	822	-	838	1366	<u>1577</u>	-

were calculated for the most stable configurations at 0.25ML. The calculated frequencies which are the closest to the experimental ones are underlined. The Raman scattering is limited to the center of the Brillion zone, and the vibrational frequencies are calculated at $\bar{\Gamma}$ point.

As shown in Fig. 5a, the frequency ω_1 (575cm^{-1} , 575cm^{-1}) (the first number stands for the experimentally measured frequency and the second one is the corresponding theoretical one, which is underlined in Table V) is the vibration of the S-C1 and the C1-C2 stretches (the O1 and O2 atoms displace slightly). The theoretical counterpart suggests that the frequency 575cm^{-1} comes from the HSCH_2COOH on the gold surface. Fig. 5b indicates that the mode ω_2 (665cm^{-1} , 670cm^{-1}) is attributed to the C1-S vibration of the SCH_2COOH on the substrate. The frequency ω_3 (763cm^{-1} , 745cm^{-1}) corresponds to the C1-S stretch of the HSCH_2COOH on the surface, where the O1 atom displaces slightly (Fig. 5c). The mode ω_4 (905cm^{-1} , 881cm^{-1}) is ascribed to the stretching vibration of the C-COOH in the HSCH_2COOH molecule on the Au(111) (Fig. 5d). ω_5 (930cm^{-1} , 929cm^{-1}) corresponds to the C-COO⁻ stretching vibration for the $\text{HSCH}_2\text{COO}^-$ on the gold surface (Fig. 5e). The frequency ω_6 (1387cm^{-1} , 1396cm^{-1}) is due to the vibration of the COOH of the SCH_2COOH on the gold surface (the C1 atom moves slightly, see Fig. 5f). The mode ω_7 (1597cm^{-1} , 1577cm^{-1}) can be assigned to this COO⁻ stretch in the SCH_2COO^- (Fig. 5g), which indicates that after the dissociation of the mercaptan hydrogen atom and the deprotonation of the carboxylic acid group, some original HSCH_2COOH molecules on the surface have

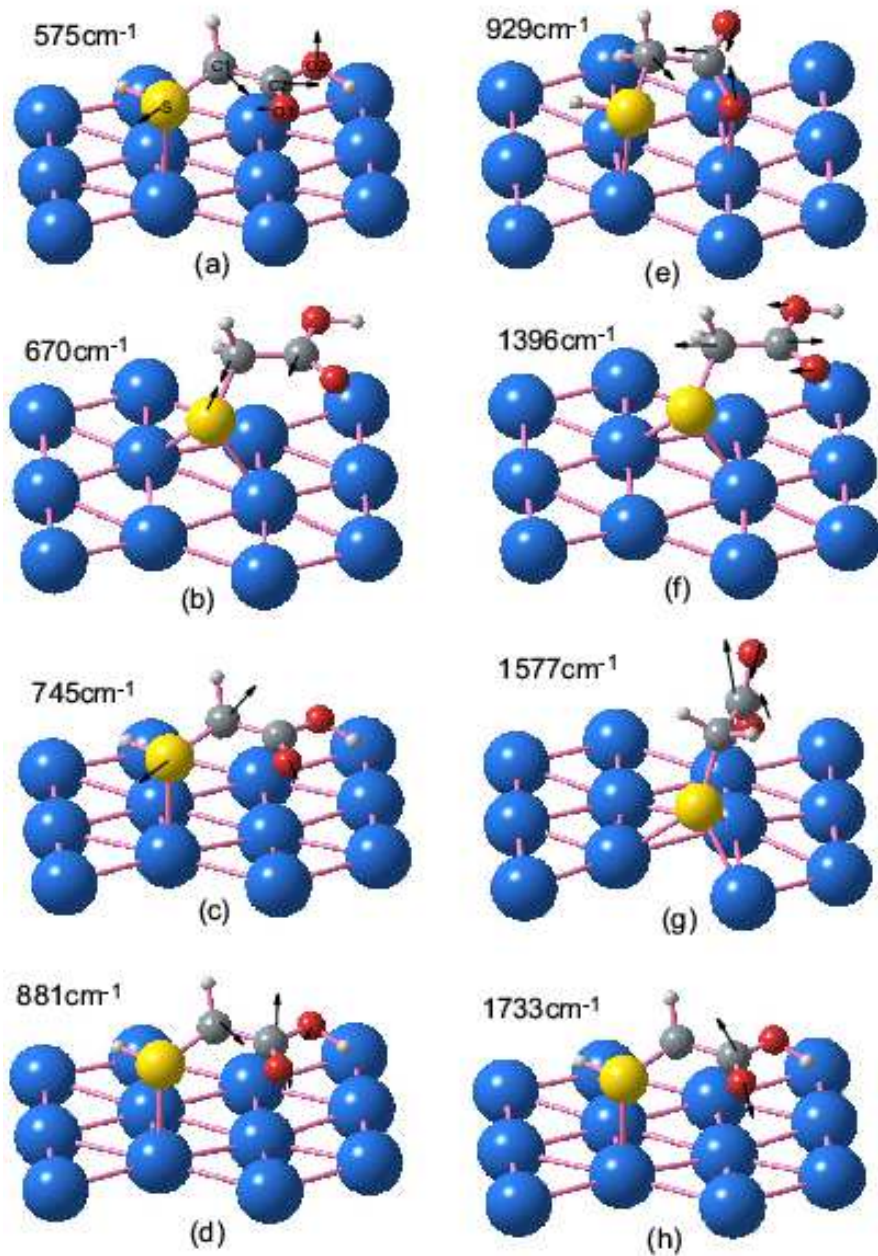


FIG. 5: (a)-(h) illustrate the calculated atomic displacements for the frequencies $\omega_1 - \omega_8$.

turned into the SCH_2COO^- molecules. The frequency ω_8 (1711cm^{-1} , 1733cm^{-1}) corresponds to the $\text{C}=\text{O}$ stretching vibration for the HSCH_2COOH on the $\text{Au}(111)$ substrate (Fig. 5h). Thus the above frequency comparison suggests that after the HSCH_2COOH molecules deposited on the $\text{Au}(111)$ surface, some stay intact on the surface, the rest have turned into SCH_2COOH (via dissociation), $\text{HSCH}_2\text{COO}^-$ (deprotonation) and SCH_2COO^- (dissociation and deprotonation).

V. CONCLUSION

We have discussed the adsorption patterns of the HSCH_2COOH , SCH_2COOH , $\text{HSCH}_2\text{COO}^-$, and SCH_2COO^- molecules on the Au(111) substrate by first-principle theoretical calculation. We have computed the partial density of states (PDOS) projected on the S and O2 atoms in the molecules on the Au(111) substrate, which display how the dissociation of the mercaptan hydrogen atom and the deprotonation of the carboxylic acid group affect the deposition and the corresponding electronic configuration. We have calculated the charge-density differences for the molecules on the Au(111) substrate, which illustrates various bonding characteristics. We have also studied the Raman vibrational spectra of the molecules adsorbed on the Au(111) substrate, and by the comparison of the experimental frequencies with the computational ones, we have identified which compounds and atomic displacements contribute to the frequencies. We have found the following adsorption mechanism for the thioglycolic acid on the Au(111) surface. Upon the HSCH_2COOH molecules deposit on the Au(111), they can either remain intact, or turn into one of the following substances: 1) SCH_2COOH in the presence of the defect on the Au(111); 2) $\text{HSCH}_2\text{COO}^-$ by increasing pH value; 3) SCH_2COO^- by the defect and increasing pH value. If the intact HSCH_2COOH is adsorbed on the gold substrate, the molecule lies down on the surface. When the SCH_2COOH molecules deposited on the Au(111) surface, some SCH_2COOH molecules lie on the substrate, but others rise up to a certain level. Thus, in the case of SCH_2COOH , different configurations may admix, and the molecules appear to be deposited on the gold substrate in a random fashion. If the carboxylic acid group in the HSCH_2COOH is deprotonated, the resulting $\text{HSCH}_2\text{COO}^-$ lies down on the surface. However, when the S-H bond in the $\text{HSCH}_2\text{COO}^-$ is broken and the molecule is turned into SCH_2COO^- , it rises up to a certain level.

Acknowledgments

This work is funded in part by the DoD (Grant No. W912HZ-06-C-0057) and DOE-BES (Grant No. DE-FG02-04ER15611).

- ¹ C. Vericat, M. Vela, G. Benitez, G. Martin, X. Torrelles, R. Salvarezza, *J. Phys.: Condens. Matter* 18, R867 (2006).
- ² K. Prime, G. Whitesides, *Science* 252, 1164 (1991).
- ³ C. Bieri, P. Ernst, S. Heyse, K. Hofmann, H. Vogel, *Nat. Biotechnol.* 17, 1105 (1999).
- ⁴ B. Houseman, J. Huh, S. Kron, M. Mrksich, *Nat. Biotechnol.* 20, 270 (2002).
- ⁵ D. Murgida, P. Hildebrandt, *J. Phys. Chem. B*105, 1578 (2001).
- ⁶ K. Ataka, J. Heberle, *J. Am. Chem. Soc.* 125, 4986 (2003).
- ⁷ M. Shimizu, K. Kobayashi, H. Morii, K. Mitsui, W. Knoll, T. Nagamune, *Biochem. Biophys. Res. Commun.* 310, 606 (2003).
- ⁸ A. Krolkowska, A. Kudelski, A. Michota, J. Bukowska, *Surf. Sci.* 532-535, 227 (2003).
- ⁹ C. Ruan, D. Yang, A. Zewail, *J. Am. Chem. Soc.* 126, 12797 (2004).
- ¹⁰ J. Lahann et al, *Science* 299, 371 (2003).
- ¹¹ I. Rzeznicka, J. Lee, P. Maksymowych, J. Yates, Jr., *J. Phys. Chem. B*109, 15992 (2005).
- ¹² J. Zhou, F. Hagelberg, *Phys. Rev. Lett.* 97, 045505 (2006).
- ¹³ J. Meyer, T. Bredow, C. Tegenkamp, H. Pfner, *J. Chem. Phys.* 125, 194705 (2006).
- ¹⁴ T. Bredow, C. Tegenkamp, H. Pfner, J. Meyer, V. Maslyuk, I. Mertig, *J. Chem. Phys.* 128, 064704 (2008).
- ¹⁵ N. Gonzalez-Lakunza, N. Lorente, A. Arnau, *J. Phys. Chem. C*111, 12383 (2007).
- ¹⁶ H. Groenbeck, H. Haekkinen, *J. Phys. Chem. B*111, 3325 (2007).
- ¹⁷ H. Groenbeck, H. Haekkinen, R. Whetten, *J. Phys. Chem. C*112, 15940 (2008).
- ¹⁸ A. Franke, E. Pehlke, *Phys. Rev. B*79, 235441 (2009).
- ¹⁹ W. Zhang, B. Gao, J.L. Yang, Z. Wu, V. Carravatta, Y. Luo, *J. Chem. Phys.* 130, 054705 (2009).
- ²⁰ P. Abufager, P. Lustemberg, C. Crespos, H. Busnengo, *Langmuir* 24, 14022 (2008).
- ²¹ G. Kresse, J. Hafner, *Phys. Rev. B*47, R558 (1993).

- ²² G. Kresse and J. Furthmüller, Phys. Rev. B54, 11169 (1996).
- ²³ G. Kresse, J. Joubert, Phys. Rev. B59, 1758 (1999).
- ²⁴ P.E. Blochl, Phys. Rev. B50, 17953 (1994).
- ²⁵ J. Perdew, Y. Wang, Phys. Rev. B46, 6671 (1992).
- ²⁶ H. J. Monkhorst, J. D. Pack, Phys. Rev. B13,5188 (1976).
- ²⁷ J. Zhou, F. Hagelberg, C. Xiao, Phys. Rev. B73, 155307 (2006); J. Zhou, Q. Williams, F. Hagelberg, Phys. Rev. B76, 075408 (2007); J. Zhou, Q. Williams, F. Hagelberg, Phys. Rev. B77, 035402 (2008).
- ²⁸ G. Makov, M. Payne, Phys. Rev. B51, 4014 (1995).
- ²⁹ A. Khein et al., Phys. Rev. B51, 4105 (1995).
- ³⁰ O. Voznyy, J. Dubowski, J. Phys. Chem. C112, 3726 (2008).
- ³¹ M. Preuss, W. Schmidt, F. Bechstedt, Phys. Rev. Lett. 94, 236102 (2005).
- ³² S. Evans, A. Ulman, Chem. Phys. Lett. 170, 462 (1990).